

# RGB and white-emitting organic lasers on flexible glass

C. Foucher,<sup>1,\*</sup> B. Guilhabert,<sup>1</sup> A. L. Kanibolotsky,<sup>2</sup> P. J. Skabara,<sup>2</sup> N. Laurand,<sup>1</sup> and M. D. Dawson<sup>1</sup>

<sup>1</sup>Institute of Photonics, Department of Physics, University of Strathclyde, Glasgow, UK

<sup>2</sup>WestCHEM, Pure and Applied Chemistry Department, University of Strathclyde, Glasgow G1 1XL, UK

\*caroline.foucher@strath.ac.uk

**Abstract:** Two formats of multiwavelength red, green and blue (RGB) laser on mechanically-flexible glass are demonstrated. In both cases, three all-organic, vertically-emitting distributed feedback (DFB) lasers are assembled onto a common ultra-thin glass membrane substrate and fully encapsulated by a thin polymer overlayer and an additional 50 $\mu$ m-thick glass membrane in order to improve the performance. The first device format has the three DFB lasers sitting next to each other on the glass substrate. The DFB lasers are simultaneously excited by a single overlapping optical pump, emitting spatially separated red, green and blue laser output with individual thresholds of, respectively, 28  $\mu$ J/cm<sup>2</sup>, 11  $\mu$ J/cm<sup>2</sup> and 32  $\mu$ J/cm<sup>2</sup> (for 5 ns pump pulses). The second device format has the three DFB lasers, respectively the red, green and blue laser, vertically stacked onto the flexible glass. This device format emits a white laser output for an optical pump fluence above 42  $\mu$ J/cm<sup>2</sup>.

©2016 Optical Society of America

**OCIS codes:** (140.0140) Lasers and laser optics; (160.4890) Organic materials; (140.3490) Lasers, distributed-feedback.

---

## References and links

1. Q. Kou, I. Yesilyurt, and Y. Chen, "Collinear dual-color laser emission from a microfluidic dye laser," *Appl. Phys. Lett.* **88**(9), 091101 (2006).
2. K. Yamashita, N. Takeuchi, K. Oe, and H. Yanagi, "Simultaneous RGB lasing from a single-chip polymer device," *Opt. Lett.* **35**(14), 2451–2453 (2010).
3. S. Omi, H. Watanabe, Y. Yang, and Y. Oki, "Development of multicolor DFB dye laser by transversal quasi-mode-coupling method," in *Conference on Lasers and Electro-Optics/Pacific Rim 2009* (Optical Society of America, 2009), paper WD2\_2.
4. F. Cornacchia, A. Di Lieto, M. Tonelli, A. Richter, E. Heumann, and G. Huber, "Efficient visible laser emission of GaN laser diode pumped Pr-doped fluoride scheelite crystals," *Opt. Express* **16**(20), 15932–15941 (2008).
5. Y. Fujimoto, O. Ishii, and M. Yamazaki, "Multi-colour laser oscillation in Pr<sup>3+</sup>-doped fluoro-aluminate glass fibre pumped by 442.6 nm GaN-semiconductor laser," *Electron. Lett.* **45**(25), 1301 (2009).
6. T. Takahashi and Y. Asami, "Hollow-cathode-type CW white light laser," *IEEE J. Quantum Electron.* **27**, 111–114 (1974).
7. Y. Shin, S. Park, Y. Kim, and J. Lee, "Development of a PC interface board for true color control using an Ar–Kr white-light laser," *Opt. Laser Technol.* **38**(4-6), 266–271 (2006).
8. S. M. Giffin, I. T. McKinnie, W. J. Wadsworth, A. D. Woolhouse, G. J. Smith, and T. G. Haskell, "Solid state dye lasers based on 2-hydroxyethyl methacrylate and methyl methacrylate co-polymers," *Opt. Commun.* **161**(1-3), 163–170 (1999).
9. S. Riechel, U. Lemmer, J. Feldmann, S. Berleb, A. G. Mückl, W. Brütting, A. Gombert, and V. Wittwer, "Very compact tunable solid-state laser utilizing a thin-film organic semiconductor," *Opt. Lett.* **26**(9), 593–595 (2001).
10. Y. Shin, S. Park, Y. Kim, and J. Lee, "Development of a PC interface board for true color control using an Ar–Kr white-light laser," *Opt. Laser Technol.* **38**(4-6), 266–271 (2006).
11. M. Kuwata, H. Sugiura, T. Sasagawa, A. Michimori, E. Toide, T. Yanagisawa, S. Yamamoto, Y. Hirano, M. Usui, S. Teramatsu, and J. Someya, "A 65-in. slim (255-mm depth) laser TV with wide-angle projection optical system," *J. Soc. Inf. Disp.* **17**(11), 875 (2009).
12. I. D. W. Samuel and G. A. Turnbull, "Organic semiconductor lasers," *Chem. Rev.* **107**(4), 1272–1295 (2007).
13. C. Foucher, B. Guilhabert, A. L. Kanibolotsky, P. J. Skabara, N. Laurand, and M. D. Dawson, "Highly-photostable and mechanically flexible all-organic semiconductor lasers," *Opt. Mater. Express* **3**(5), 584 (2013).

14. C. Foucher, B. Guilhabert, N. Laurand, and M. D. Dawson, "Wavelength-tunable colloidal quantum dot laser on ultra-thin flexible glass," *Appl. Phys. Lett.* **104**(14), 141108 (2014).
15. A. L. Kanibolotsky, F. Vilela, J. C. Forgie, S. E. T. Elmasly, P. J. Skabara, K. Zhang, B. Tieke, J. McGurk, C. R. Belton, P. N. Stavrinou, and D. D. C. Bradley, "Well-defined and monodisperse linear and star-shaped quaterfluorene-DPP molecules: the significance of conjugation and dimensionality," *Adv. Mater.* **23**(18), 2093–2097 (2011).
16. A. Rose, Z. Zhu, C. F. Madigan, T. M. Swager, and V. Bulović, "Sensitivity gains in chemosensing by lasing action in organic polymers," *Nature* **434**(7035), 876–879 (2005).
17. Y. Chen, J. Herrnsdorf, B. Guilhabert, A. L. Kanibolotsky, A. R. Mackintosh, Y. Wang, R. A. Pethrick, E. Gu, G. A. Turnbull, and P. J. Skabara, "Laser action in a surface-structured free-standing membrane based on a  $\pi$ -conjugated polymer-composite," *Org. Electron.* **12**(1), 62–69 (2011).
18. G. Tsiminis, Y. Wang, P. E. Shaw, A. L. Kanibolotsky, I. F. Perepichka, M. D. Dawson, P. J. Skabara, G. Turnbull, and I. D. W. Samuel, "Low-threshold organic laser based on an oligofluorene truxene with low optical losses," *Appl. Phys. Lett.* **94**(24), 243304 (2009).
19. A. L. Kanibolotsky, R. Berridge, P. J. Skabara, I. F. Perepichka, D. D. C. Bradley, and M. Koeberg, "Synthesis and properties of monodisperse oligofluorene-functionalized truxenes: highly fluorescent star-shaped architectures," *J. Am. Chem. Soc.* **126**(42), 13695–13702 (2004).
20. C. Foucher, B. Guilhabert, J. Herrnsdorf, N. Laurand, and M. D. Dawson, "Diode-pumped, mechanically-flexible polymer DFB laser encapsulated by glass membranes," *Opt. Express* **22**(20), 24160–24168 (2014).
21. O. G. Abdullah and D. R. Saber, "Optical absorption of polyvinyl alcohol films doped with nickel chloride," *Appl. Mech. Mater.* **110**(116), 177–182 (2011).
22. C.-Y. Sun, X.-L. Wang, X. Zhang, C. Qin, P. Li, Z.-M. Su, D.-X. Zhu, G.-G. Shan, K.-Z. Shao, H. Wu, and J. Li, "Efficient and tunable white-light emission of metal-organic frameworks by iridium-complex encapsulation," *Nat. Commun.* **4**, 2717 (2013).

## 1. Introduction

Compact multicolour laser sources are attractive for many applications, for example optoelectronics, chemical reaction control, micro-total analysis and sensing [1–3]. Gas lasers or solid-state lasers (Ti:Sapphire lasers, for example) can be used as multiwavelength laser sources. RGB lasers have been demonstrated with a  $\text{Pr}^{3+}$ -doped fluoride glass fibre or crystal [4,5], a hollow-cathode He–Cd laser [6] and an Ar–Kr mixed gas laser [7]. However, these systems are often expensive and bulky and are ill-suited for integrated devices [3,8–10]. Semiconductor laser diodes are compact but the heterogeneous integration of several wavelengths comes with a high cost and it is still difficult to access certain wavelengths like in the green-orange region of the visible [11].

Organic semiconductor (OS) materials are a good alternative for multiwavelength lasers because they can be tailored to cover the whole visible spectrum, e.g. allowing a selection of wavelengths according to the application [12], and their fabrication is simple and rapid using soft lithography and solution-processing techniques [13]. This simplicity of fabrication enables a wide range of device structures as well as conformation and mechanical flexibility. The challenge though is how to combine different laser materials and structures so that stable simultaneous multi-wavelength emission is obtained with a single pump source.

In this paper, we report two types of RGB laser integrated on ultra-thin flexible glass. The first device is a multicolour laser array consisting of three individual lasers (red, green and blue or RGB) juxtaposed onto the flexible glass substrate. The second device is made of three independent RGB lasers vertically integrated on top of each other onto the flexible glass. In the latter, the outputs of the individual lasers inherently combine to give a white light emission. In both device formats, the OS laser materials are fully encapsulated by a combination of transparent polymer and flexible glass. In the following, section 2 explains the design and fabrication process of these two formats of RGB laser. In section 3, equivalent individual red, green and blue lasers made of non-encapsulated, neat OS materials are independently characterised to serve as references for the discussion of section 4. Finally, section 4 presents and discusses the experimental results, including spectra and power transfer functions for both RGB device configurations.

## 2. Design and fabrication

### 2.1 The two RGB laser formats

Figure 1 (a) represents the structure of the first RGB laser format. This structure is called the “line” configuration in the rest of the paper. It is formed by three individual DFB lasers made of a gain layer (~180 nm-thick for the red laser, ~130 nm for the green laser and ~75 nm for the blue laser) deposited on top of a ~43  $\mu\text{m}$ -thick epoxy grating with a 40 nm modulation depth. The periodicity of the grating is chosen to yield a second-order DFB cavity with a vertical emission due to first-order diffraction [14]. The lasers are assembled manually, adjacent to each other, onto a 50  $\mu\text{m}$ -thick flexible glass substrate (AF32 glass). In this configuration, the R, G and B lasers are excited simultaneously with an overlapping pump stripe ( $1.8 \times 15.3 \text{ mm}^2$  FWHM). The gain material of the red laser is 1,4-diketo-2,3,5,6-tetraphenyl-pyrrolo[3,4-c]pyrrole (linear-c DPP), a monodispersed  $\pi$ -conjugated oligomer with an emission spectrum that spans the 530-600 nm region and an absorption that peaks at 365 nm [15]. The green laser material is  $\pi$ -conjugated poly[2,5-bis(2',5'-bis(2''-ethylhexyloxy)phenyl)-p-phenylene vinylene] (BBEHP-PPV) with emission spanning the 490-540 nm spectral region and absorption centred at 430 nm [16,17]. The blue laser material is a star-shaped tris(terfluorenyl) based on a truxene core (T3), an oligomer whose main luminescence is around 420-470 nm with absorption peaking at 375 nm [18,19]. Once assembled onto the flexible glass substrate, these individual lasers are encapsulated with a protective 180 nm-thick layer of polyvinyl alcohol (PVA) and a second 50  $\mu\text{m}$ -thick flexible glass sheet. The total thickness of the RGB sample is <150  $\mu\text{m}$  and its area is ~1.2  $\text{cm}^2$ .

The second format of RGB laser, shown in Fig. 1 (b), is formed by the three R, G and B lasers described above, stacked on top of each other (instead of being placed next to each other). PVA and epoxy layers separate each laser. The DFB cavities are therefore vertically spaced by >43  $\mu\text{m}$ , preventing any undesirable mode coupling between them. Hence, the DFB lasers oscillate independently, which enables stable multi-wavelength operation from the overall device. As shown in Fig. 1 (b), the order in which the DFB lasers are stacked means that the pump is absorbed first by the blue laser, then the green and finally the red. The reason for this order is to minimise the differences in optical density and oscillation thresholds of the T3, BBEHP-PPV and linear-c DPP lasers. Throughout the paper, this device format is called the “stack”. Under optical pumping, each DFB laser emits simultaneously, their output overlapping, thereby giving a combined white emission. The whole RGB device is encapsulated with a second 50  $\mu\text{m}$ -thick flexible glass membrane. The total thickness of the device is <250  $\mu\text{m}$ .

The encapsulation of both devices with glass membranes retains the bendability and should improve the operational lifetime as it has been demonstrated before for a BBEHP-PPV DFB laser encapsulated with thin-glass [20]. The lasers were optically pumped with pulse excitation of a few nanoseconds in duration (from a Q-switch laser) in order to prevent triplet build-up. We note that such pulse duration is readily achievable with InGaN laser diode and light emitting diodes.

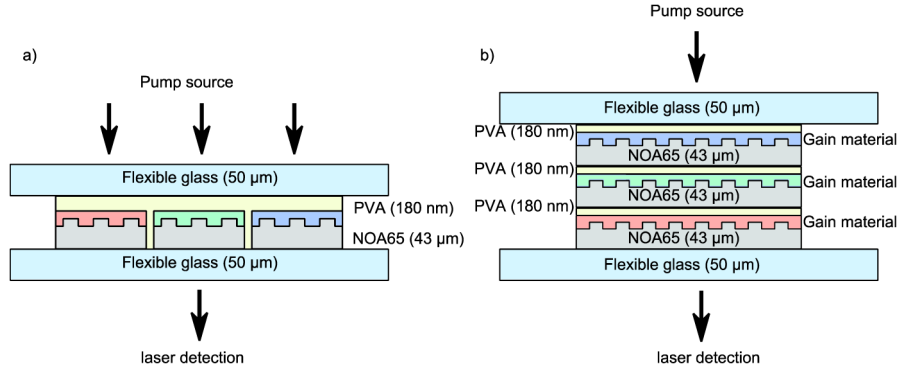


Fig. 1. Structure of the two RGB devices with a) the “line” design and b) the “stack” design. The arrows indicate the incident pump and the RGB laser output.

## 2.2 Fabrication steps

For both device formats, the red, green and blue lasers are vertically-emitting DFB lasers. They are fabricated individually before being assembled together onto the thin glass substrate. Their cavities are fabricated by soft-lithography, reproducing a glass master grating with a UV curable epoxy (NOA65), using the same method as in [13]. The appropriate period is chosen for each master grating to yield a second order distributed feedback cavity: 390 nm for the red emitting material, 350 nm for the green and 276 nm for the blue.

Each gain material is diluted in toluene at a chosen concentration and spin-coated on top of the corresponding grating. A solution of 50 mg/mL of linear-c DPP is spin-coated at 5000 rpm, 20 mg/mL of BBEHP-PPV at 5000 rpm and 20 mg/mL of T3 at 3200 rpm in order to form a gain layer thickness that ensures good confinement of the transverse mode: ~120 nm for linear-c DPP, ~130 nm for BBEHP-PPV and ~75 nm for T3.

For the “line” device, each laser is then cut into squares of  $0.4 \times 0.4 \text{ cm}^2$ . A drop of NOA65 (epoxy) is spin-coated at 8000 rpm on top of the 50  $\mu\text{m}$ -thick flexible glass substrate before each laser is deposited onto it. This is followed by a photocuring step under a UV flooding for a total exposure dose of  $300 \text{ mJ/cm}^2$ . The structure of assembled lasers is then overcoated with a 180 nm-thick layer of PVA, prepared from a 50 mg/mL solution in deionised water and spin-coated at 3200 rpm. A second glass membrane is placed on top of the PVA layer and sealed to the other glass sheet using NOA65 at the edge. A final UV dose of  $300 \text{ mJ/cm}^2$  is applied. The device is finally annealed in air for three days at  $35^\circ\text{C}$ .

For the “stack” device format, each individual laser is overcoated with a 180 nm thick layer of PVA before they are assembled together. Again, a drop of NOA65 is spin-coated at 8000 rpm on top of the 50  $\mu\text{m}$ -thick flexible glass substrate. The red emitting laser is deposited on the substrate first, and the two others are stacked on top of the red one as depicted in Fig. 1(b). The second glass sheet is added on top of the blue laser to seal the structure as detailed above. The whole device is also annealed for three days at  $35^\circ\text{C}$  [21].

## 3. Individual neat reference lasers

Neat lasers made only of a pure film of OS on top of an epoxy grating, with no overlayer or encapsulation, were fabricated and used as references for performance comparison when the encapsulation is applied. They were optically pumped by a Q-switched, frequency-tripled Nd:YAG laser emitting 5 ns pulses at a wavelength of 355 nm and with a 10 Hz repetition rate. The laser emission was detected by a 50  $\mu\text{m}$ -core optical fibre, connected to a CCD-spectrometer with a spectral resolution of 0.13 nm [13]. The spectrometer detector response was normalised using an intensity-calibrated white light source (HL2000, Ocean Optics). The average threshold energy fluence per pulse,  $F_{\text{th}}$ , of a neat red, green and blue laser was measured.

The neat linear-c DPP laser emitted at 603.2 nm and had an  $F_{th}$  of 168  $\mu\text{J}/\text{cm}^2$ . The neat BBEHP-PPV laser emitted at 536.5 nm and its  $F_{th}$  was found to be 239  $\mu\text{J}/\text{cm}^2$ . Finally, the neat T3 laser had an emission wavelength of 426.3 nm and an  $F_{th}$  of 70  $\mu\text{J}/\text{cm}^2$ . Spectra and power transfer functions are given for T3 in Fig. 2 (a), BBEHP-PPV in Fig. 2 (b) and linear-c DPP in Fig. 2 (c), respectively. The broad spectrum of the neat T3 laser (1.5 nm) compared to the neat green and red lasers (respectively of 0.25 nm and 0.40 nm) is probably due to a multimode emission for this particular laser, engendered by a defect in the structure of the gain material thin-film or in the grating at the pumping position. However, many neat T3 lasers have been tested for this experiment and a linewidth of 0.3 nm under the same conditions was generally obtained.

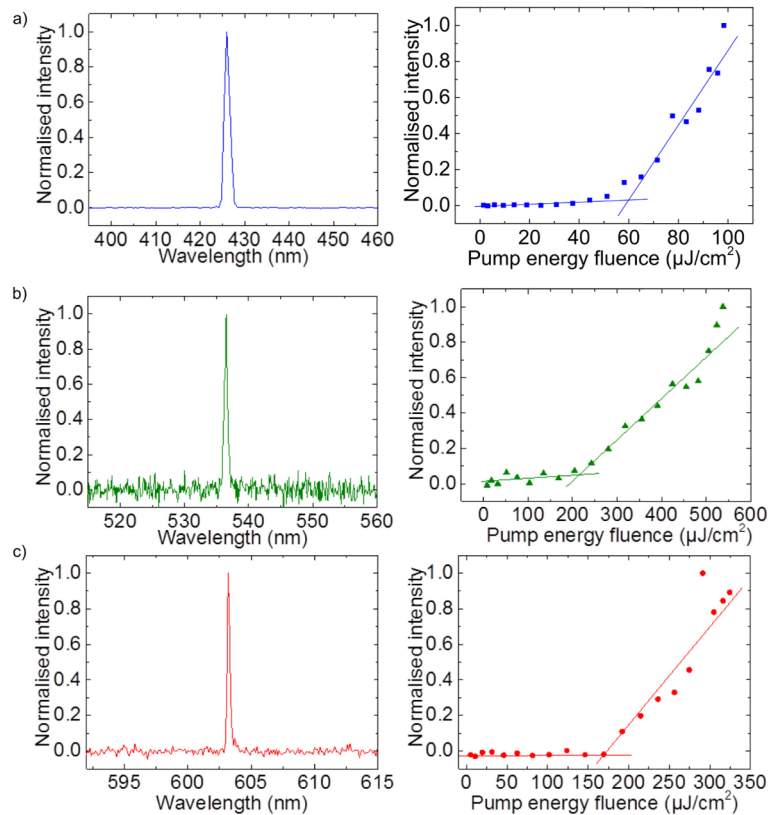


Fig. 2. Spectra and power transfer functions of a) neat T3 laser, b) neat BBEHP-PPV laser and c) neat linear-c DPP laser.

#### 4. RGB laser characteristics

The RGB devices were characterised in the same manner as the reference lasers.

##### 4.1 “Line” configuration device

The spectrum of the “line” RGB laser is shown in Fig. 3 (a) when above threshold at a pump energy fluence of 38  $\mu\text{J}/\text{cm}^2$ . A picture of the emitted beams is shown in Fig. 3 (c). As the emission of the DFB lasers making the line device are separated spatially, each output beam is measured independently. The reader is reminded that the device is pumped with a single pump stripe covering the whole device that emits at 3 wavelengths: 605.4 nm, 537.1 nm and 435.9 nm. Results show that the encapsulating layers (PVA plus thin glass) redshift the oscillation wavelengths compared to the reference lasers (603.2 nm, 536.5 nm and 426.3 nm).

The encapsulating layers change the refractive index profile of the laser structure and as a result the effective refractive index of the mode increases [13].

The threshold fluences of the devices are measured and plotted in Fig. 3 (b). The green emitting laser has the lowest threshold,  $11 \mu\text{J}/\text{cm}^2$ , followed by the red laser with an average threshold fluence of  $28 \mu\text{J}/\text{cm}^2$  and the blue laser with an average threshold of  $31 \mu\text{J}/\text{cm}^2$ . It is seen that the encapsulation lowers considerably the threshold compared to the equivalent neat lasers, (respectively  $168 \mu\text{J}/\text{cm}^2$ ,  $239 \mu\text{J}/\text{cm}^2$  and  $70 \mu\text{J}/\text{cm}^2$ ), also attributed to changes in the refractive index profile of the laser structure, increasing the modal overlap in the gain region and possibly mitigating the effect of scattering loss at the laser interfaces. However, the difference in improvement between each material could be explained by the different overlap improvements, as they depend on the thickness of the gain material. The intensity profile of the pump follows a Gaussian power distribution and the difference in  $F_{\text{th}}$  between each laser can also be explained by this Gaussian distribution: the green laser is directly under the Gaussian peak of the intensity distribution while the red and blue are on the side of the stripe. However a top-hat lens can in principle be used to transform this Gaussian distribution into a flat distribution.

One can notice the switching of the colours in Fig. 3 (c). This could be induced by the manual positioning of each laser causing issues in terms of placement and angular misalignment. A future plan would be to use transfer printing, for example, to ensure a more precise and repetitive process.

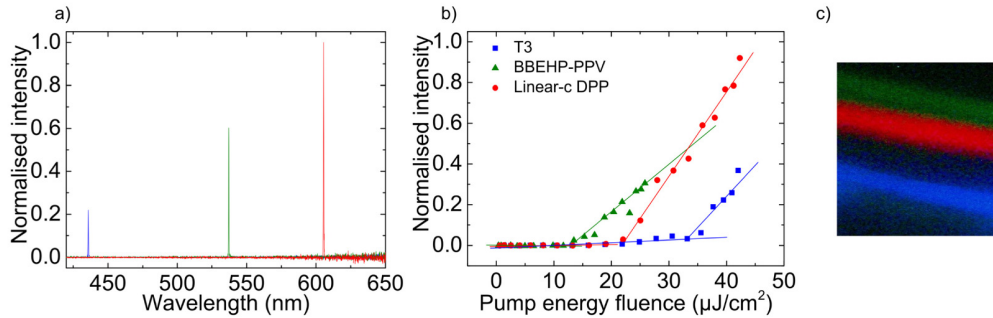


Fig. 3. a) Spectrum, b) pump energy fluence and c) photograph of the “line” RGB.

#### 4.2- “Stack” configuration device

Figure 4 shows the characteristics of the “stack” RGB laser. From Fig. 4 (a) it is seen that the laser emits simultaneously at three different wavelengths: 608.3 nm, 540.1 nm and 435.9 nm (measured at a pump fluence of  $55 \mu\text{J}/\text{cm}^2$ ). The three beams, red, green and blue emit from the same position on the sample, giving a quasi-white light emission. As seen previously, a red shift in wavelength is caused by the encapsulation, compared to equivalent neat lasers ( $603.2 \text{ nm}$ ,  $536.5 \text{ nm}$  and  $426.3 \text{ nm}$  emission). A picture of the device under optical pumping is shown in Fig. 4 (c).

The power transfer function of the RGB laser is shown in Fig. 4 (b). It can be seen that the individual oscillation thresholds in terms of incident energy fluence increase for the G and R lasers compared to the line device. This is expected as the pump excites first the B laser and is depleted as it travels through the structure. However, these thresholds are still highly reduced, because of the encapsulation, compared to the equivalent neat lasers. The whole device threshold is then  $42 \mu\text{J}/\text{cm}^2$  (when the three lasers emit at the same time). This is an improvement in threshold of  $\sim 100$  times compared to the result shown by Yamashita et al. [2]. However, there is a slight increase in threshold compared to the “line” device due to the configuration of the device as the laser on top of another laser acts as a superstrate.

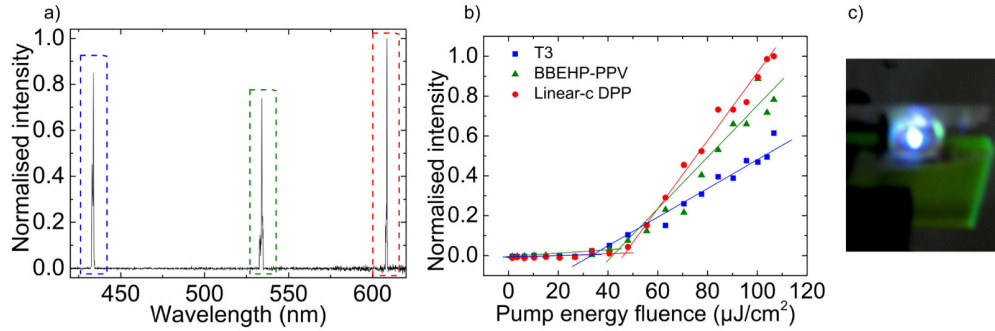


Fig. 4. a) Spectrum, b) pump energy fluence and c) photograph of the “stack” RGB laser.

## 5. Chromaticity study

The CIE coordinates of the “stack” laser configuration are calculated in order to deduce the colour of laser emission. Figure 5 (a) plots the evolution of the emission spectra and peak intensity against the increase of the pumping fluence.

The CIE coordinates are determined for fluences of 45, 50, 55, 60, 65, 70, 75 and 80  $\mu\text{J}/\text{cm}^2$ , respectively, and are plotted in Fig. 5 (b). “1” represents the coordinates for 45  $\mu\text{J}/\text{cm}^2$  pump energy fluence, “2” for 50  $\mu\text{J}/\text{cm}^2$ , “3” for 55  $\mu\text{J}/\text{cm}^2$  and “4” for a pump fluence  $>60 \mu\text{J}/\text{cm}^2$  (the coordinates do not change significantly above 60  $\mu\text{J}/\text{cm}^2$ ). One can see that white emission is obtained for this device when pumped above threshold. As an example the calculated CIE coordinates are: (0.33, 0.27, 0.39) as plotted in Fig. 5 (b), point “3” (corresponding to the spectrum in Fig. 4 (a)).

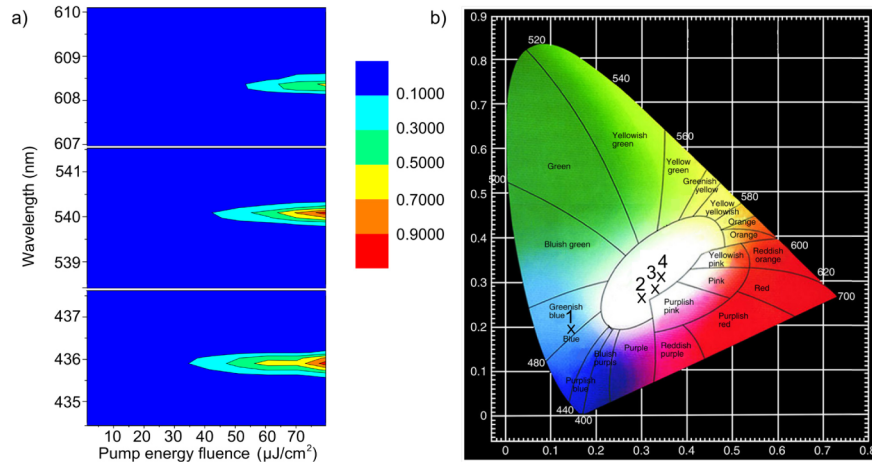


Fig. 5. a) Evolution of the emission spectra of the “stack” laser configurations and b) CIE chromaticity diagram with the CIE coordinates of the “stack” RGB lasers [22].

## 6. Conclusion

In summary, two formats of mechanically-flexible RGB lasers on an ultra-thin glass substrate are demonstrated, one being a multicolour laser array and the other a single-chip white laser. Both devices are fabricated by combining three individual all-organic DFB lasers entirely made by soft lithography. The complete devices are encapsulated with polymer and an additional 50  $\mu\text{m}$ -thick glass membrane. The multicolour laser array device consists of three DFB lasers placed next to each other on the flexible glass substrate. Each laser is optically-pumped simultaneously, giving a red, green and blue laser output with an individual threshold of, respectively, 28  $\mu\text{J}/\text{cm}^2$ , 11  $\mu\text{J}/\text{cm}^2$  and 32  $\mu\text{J}/\text{cm}^2$ . The second device, the white emission

laser, has the three red, green and blue DFB lasers vertically stacked. The output of the individual DFB lasers combines to give a white laser emission for a threshold of  $42 \mu\text{J}/\text{cm}^2$ . These demonstrations offer potential solutions for the development of compact multicolour and white light laser sources. This opens opportunities for chemical, biological analysis, sensors and many other optoelectronics applications.

### **Acknowledgments**

The authors would like to thank the Engineering and Physical Sciences Research Council for funding under the grant EP/J021962/1, Hybrid Colloidal Quantum Dot Lasers for Conformable Photonics, HYPIX and PJS thanks the Royal Society for a Wolfson Research Merit Award.